Charged-particle multiplicity distributions in pp, $\pi^{\pm}p$, and $K^{\pm}p$ collisions and $e^{+}e^{-}$ and $\bar{p}p$ annihilations

Y. K. Lim and K. K. Phua
Physics Department, National University of Singapore, Singapore 0511
(Received 5 March 1981; revised manuscript received 27 October 1981)

A mixed two-component model is used to fit the available charged-particle multiplicity distribution from pp, $\pi^{\pm}p$, and $K^{\pm}p$ collisions and $e^{+}e^{-}$ and $\bar{p}p$ annihilations. Generally good agreement is obtained between theory and experiment with respect to the dispersion, and second, third, and fourth normalized moments. Koba-Nielsen-Olesen scaling is seen to hold approximately in this model.

I. INTRODUCTION

The charged-particle multiplicity distribution has been extensively measured and studied for pp collisions for beam momenta up to 405 GeV/c (Ref. 1) and for intersecting-storage-ring (ISR) energies[2] up to 63 GeV. Inelastic topological cross sections for $\pi^{\pm}p$ and $K^{\pm}p$ collisions have also been reported for somewhat lower beam momenta.[3] One remarkable feature that has emerged is that Koba-Nielsen-Olesen (KNO) scaling[4] appears to hold at least approximately.[2,5] Thus the inelastic topological cross sections plotted in the form of $\langle n\rangle\sigma_n/\sigma_{\text{inel}}$ against $n/\langle n\rangle$ (where σ_n is the partial inelastic cross section for the reaction $hh\rightarrow n$ charged particles, σ_{inel} the total hadron-hadron inelastic cross section, and $\langle n\rangle$ the mean charged-particle multiplicity) appear to be independent of the incident energy.

Recently, the topological cross sections for $e^{+}e^{-}$ annihilations have become available for certain ISR energies and KNO scaling again appears to be valid,[6] albeit the KNO plots for pp collisions and for $e^{+}e^{-}$ annihilations differ significantly. The $\bar{p}p$-annihilation topological cross sections are more uncertain as at large energies the $\bar{p}p$ inelastic scattering channels become significant. To a first approximation, the difference between the $\bar{p}p$ and pp topological cross sections at the same beam momentum may be considered as the $\bar{p}p$ annihilation cross section.[7] It has been noted that the KNO plots for the $e^{+}e^{-}$ and the $\bar{p}p$ annihilations are remarkably similar.[6]

In this paper is presented an analysis of the pp, $\pi^{\pm}p$, and $K^{\pm}p$ inelastic, and $e^{+}e^{-}$ and $\bar{p}p$ annihilation topological cross sections using the extension of a semiempirical mixed two-component (MTC) model first proposed by Kam, Low, and Phua[8] for fitting the multiplicity distribution of negatively charged particles emitted in pp collisions.

II. THE MIXED TWO-COMPONENT MODEL

It is supposed that as the two colliding hadrons pass through each other energy is dissipated in a central region, where pionization subsequently takes place, while each hadron becomes excited and fragments. The particles arising from pionization and from fragmentation are assumed to be produced independently in so far as charge conservation allows. The probability for producing n charged particles in a collision is then the sum of the products of the probabilities for producing n_c charged particles by pionization and n_f charged particles by fragmentation where $n_c+n_f=n$:

$$P(n)=2\sum_{n=n_c+n_f}{}' Q(n_c)F(n_f)\,. \tag{1}$$

Note that charge conservation requires that $\sum'$ sums over even values of n only, i.e., $n=2,4,6,\ldots$, and the missing terms are compensated by the factor 2. The pionization process is assumed to be random and to follow a Poisson distribution

$$Q(n_c)=\exp(-m)\frac{m^{n_c}}{n_c!}\,, \tag{2}$$

where m is the mean number of charged particles arising from pionization.

Studies of high-mass diffractive dissociation, in which one proton is quasielastically scattered while the other is excited and fragments into particles, at the CERN ISR have shown that the excitation spectrum has a M^{-2} dependence, where M is the "missing mass," up to $M\sim 5$ GeV, after which the differential cross section levels off.[9] This sug-

gests[10] a simple n^{-2} distribution for fragmentation multiplicity n. To allow for the presence of a leading particle we use the expression $(n+k)^{-2}$, where K is a constant for a given collision energy, for the relative probability of finding n charged fragments from an excited hadron. Consider for example the simple case of an excited proton fragmenting into $n-1$ charged pions and a leading proton, all having the same velocity. We would have

$$M \propto [3(n-1)/2 + m_p/m_\pi] \propto [n + (2m_p/3m_\pi - 1)] .$$

Furthermore, an energy-dependent cutoff is imposed on the number of such fragments.

In the case of a meson-proton collision we recognize the fact that the two excited hadrons are likely to be different in their fragmentation properties. Thus in general the excited hadrons are assumed to fragment with distributions $(n_f+K_1)^{-2}$ and $(n_f+K_2)^{-2}$, and subject to cutoffs N_1 and N_2, respectively.

Only one or both of the excited hadrons may fragment. If D is the probability of a hadron fragmenting and $E=1-D$, then the relative probabilities of elastic scattering, single, and double fragmentation are E^2, $2ED$, and D^2, respectively. E^2 is thus the ratio of the elastic to the total cross section, and the probability of single fragmentation occurring is

$$p = \frac{2ED}{2ED+D^2} . \tag{3}$$

The probability of producing n_f charged fragments in a collision is therefore

$$F(n_f) = \frac{p}{k_1} F_1(n_f) + \frac{1-p}{k_2} \sum_{n_f=n_R+n_L} F_2(n_R,n_L) , \tag{4}$$

where

$$F_1(n_f) = \begin{cases} \frac{1}{2}[(n_f+K_1)^{-2}+(n_f+K_2)^{-2}] & \text{for } 0 \le n_f \le N_1 , \\ (n_f+K_2)^{-2} & \text{for } N_1 < n_f \le N_2 , \\ 0 & \text{for } N_2 < n_f , \end{cases}$$

$$F_2(n_R,n_L) = \begin{cases} (n_R+K_1)^{-2}(n_L+K_2)^{-2} & \text{for } 0 \le n_R+n_L \le N_1+N_2 , \\ 0 & \text{otherwise} , \end{cases}$$

n_R and n_L being the numbers of charged fragments from the "right" and "left" excited hadrons, respectively, k_1 and k_2 are normalization constants:

$$k_1 = \sum_{n_f=0}^{N_2} F_1(n_f) ,$$

$$k_2 = \sum_{n_f=0}^{N_1+N_2} \sum_{n_f=n_R+n_L} F_2(n_R,n_L)$$

and p is the probability of only one excited hadron fragmenting given by Eq. (3). Note that in the above we have taken N_2 to be greater than or equal to N_1.

The mean number of charged fragments is then

$$S = \sum_{n_f=0}^{N_1+N_2} n_f F(n_f) , \tag{5}$$

whence the mean number of charged particles form the pionization of the central region

$$m = \langle n \rangle - S , \tag{6}$$

$\langle n \rangle$ being the experimental mean charged-particle multiplicity.

The model in general contains four parameters K_1, K_2, N_1, and N_2 and requires the input of the experimental mean multiplicity $\langle n \rangle$. For comparison with experiments it is convenient to present the theoretical distribution in the form of KNO plots, i.e., $\langle n \rangle P(n)$ versus $n/\langle n \rangle$. For our calculations we have used a value 0.20 for the ratio elastic to total cross section for hadron collisions[11] which gives $p=0.618$. The theoretical distributions in the form of KNO plots have been found to be quite insensitive to the variations of the parameters p, K_1, K_2, N_1, and N_2.

III. CHARGED-PARTICLE MULTIPLICITY DISTRIBUTION IN *pp* COLLISIONS

For *pp* collisions the model requires that $K_1=K_2\equiv K$. A cutoff N is imposed on the number of charged particles from double fragmentation and a cutoff $N/2$ [or $(N+1)/2$, whichever is an

integer] is imposed on single fragmentation. The number of free parameters is thus reduced to two. The pp-collision inelastic topological cross sections[1] for beam momenta above 50 GeV/c are fitted by the following procedure. For each experiment the values of the parameters K and N are found for which the mean χ^2 per data point falls in the range of smallest values. Only data points which have been based on four or more observed events or which are stated to have errors better than 50% are included in the χ^2 computation. The calculated distribution for such values of K and N which best matches the calculated and experimental values of the dispersion

$$D=(\langle n^2\rangle-\langle n\rangle^2)^{1/2}$$

is considered to be the best fit. The results are given in Table I, where the theoretical and experimental values of the normalized moments C_2, C_3, and C_4, defined by

$$C_q=\frac{\langle n^q\rangle}{\langle n\rangle^q},$$

are also compared.

The fit is generally good as can be seen from the agreement between the theoretical and experimental values of the dispersion and normalized moments. The χ^2's are quite reasonable except for three experiments where χ^2 per point exceeds 3. One case, namely that for beam momentum 405 GeV/c, has χ^2/point$\sim$9. It reduces to $\sim$4 however if the data point for $n=2$ is excluded from the χ^2 computation.

The parameter K appears to increase slowly with energy. However, a common value $K=6$ would be able to fit all the data with only marginal sacrifice in the goodness of fit.

Figure 1 shows two examples of the fitting curves, presented as KNO plots, corresponding to the lowest and highest energies fitted. It is interesting to note that whereas KNO scaling is not valid it holds approximately in our model.

IV. CHARGED-PARTICLE MULTIPLICITY DISTRIBUTION IN e^+e^- AND $\bar{p}p$ ANNIHILATIONS

To apply the MTC model to annihilations, we again suppose that as the particle and antiparticle come into collision energy is dissipated in the central region where pionization subsequently takes place. The annihilation itself produces two fireballs which fragment into mesons. Two modifications are then to be made to the model: As there is no leading particle, $K_1=K_2=0$, and as fragmentation must take place for both fireballs, $p=0$. For the fragmentation cutoffs, we set $N_1=N_2=N$ so that only one free parameter remains.

The result of fitting the e^+e^- annihilation data of PLUTO Collaboration[6] at ISR energies of 9.4 GeV and 29.9–31.6 GeV is shown in Table II and

TABLE I. pp collisions. Experimental data from Refs. 1 and 2.

Author	Beam momentum or ISR energy	$\langle n\rangle$	K	N	Dispersion D Expt.	Theor.
Ammosov *et al.*	50 GeV/c	5.32±0.13	5	6	2.58±0.05	2.54
Bromberg *et al.*	60 GeV/c	5.60±0.09	5	6	2.56±0.06	2.60
Ammosov *et al.*	69 GeV/c	5.89±0.07	5	8	2.89±0.03	2.90
Morse *et al.*	100 GeV/c	6.37±0.06	5	10	3.26±0.05	3.26
Erwin *et al.*	100 GeV/c	6.49±0.10	5	10	3.28±0.09	3.28
Chapman *et al.*	102 GeV/c	6.34±0.14	5	10	3.19±0.08	3.25
Bromberg *et al.*	102 GeV/c	6.32±0.07	5	9	3.13±0.04	3.10
Charlton *et al.*	205 GeV/c	7.65±0.17	5	13	3.88±0.13	3.90
Dao *et al.*	303 GeV/c	8.86±0.16	6	15	4.38±0.10	4.41
Bromberg *et al.*	405 GeV/c	8.99±0.14	6	17	4.75±0.09	4.75
Thomé *et al.*	ISR 24 GeV	8.12±0.08	6	13	4.05±0.08	4.00
Thomé *et al.*	ISR 31 GeV	9.54±0.12	6	17	4.83±0.13	4.81
Thomé *et al.*	ISR 45 GeV	11.01±0.17	6	23	5.90±0.18	5.96
Thomé *et al.*	ISR 53 GeV	11.7 ±0.10	6	25	6.39±0.02	6.35
Thomé *et al.*	ISR 63 GeV	12.7 ±0.12	7	27	6.92±0.13	6.87

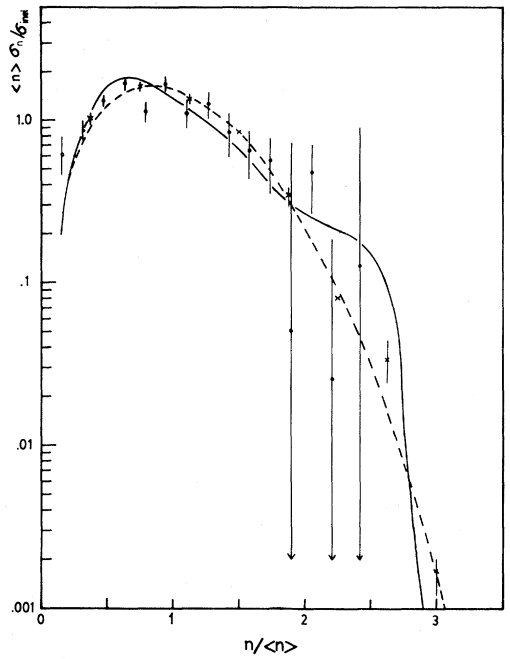

FIG. 1. KNO plots for pp collisions. Experimental points: × 50 GeV/c, ● 63 GeV ISR. Theoretical curves: dashed 50 GeV/c, solid 63 GeV ISR.

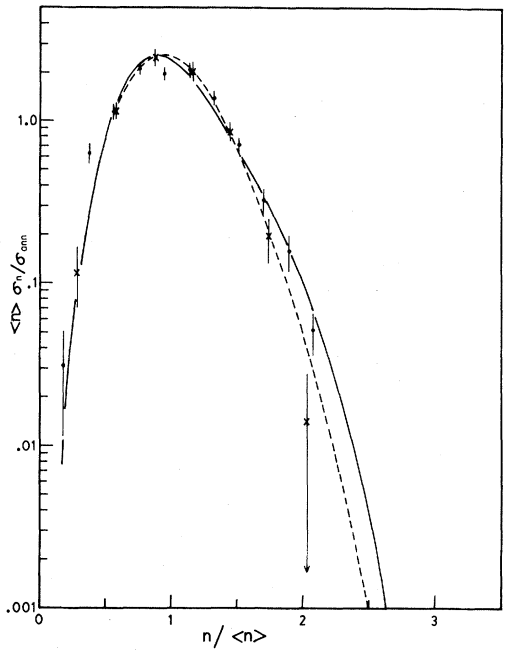

FIG. 2. KNO plots for e^+e^- annihilations, σ_{ann} being the total annihilation cross section. Experimental points: × 9.4 GeV ISR, ● 29.9–31.6 GeV ISR. Theoretical curves: dashed 9.4 GeV ISR, solid 29.9–31.6 GeV ISR.

Fig. 2. The fit is generally good, though for the high energy data, the χ^2 square value is rather high (4 per point).

Rushbrooke *et al.*[7] have compiled the annihilation topological cross sections for $\bar{p}p$ collisions, taken as the difference between $\bar{p}p$ and pp cross sections, for beam momenta up to 100 GeV/c. Their graph has been reproduced as Fig. 3 together

TABLE I. *(Continued.)*

C_2		C_3		C_4		
Expt.	Theor.	Expt.	Theor.	Expt.	Theor.	χ^2/point
1.23 ±0.04	1.23	1.75±0.08	1.74	2.89±0.17	2.73	6.1/7
1.21 ±0.05	1.21	1.68±0.09	1.69	2.60±0.19	2.61	1.8/7
1.24 ±0.02	1.24	1.79±0.04	1.79	2.97±0.08	2.88	13/8
1.26 ±0.03	1.26	1.87±0.05	1.87	3.10±0.11	3.12	32.1/9
1.26 ±0.04	1.25	1.85±0.07	1.84	3.09±0.16	3.05	10/8
1.26 ±0.06	1.26	1.85±0.11	1.87	3.07±0.22	3.13	5.5/9
1.24 ±0.03	1.24	1.81±0.05	1.79	2.98±0.11	2.87	14.1/9
1.26 ±0.04	1.26	1.85±0.07	1.87	3.06±0.15	3.14	28.8/10
1.25 ±0.05	1.25	1.82±0.09	1.83	2.98±0.19	3.02	28.9/11
1.28 ±0.03	1.28	1.96±0.08	1.96	3.42±0.20	3.40	113/12
1.249±0.009	1.241	1.84±0.03	1.80	3.08±0.09	2.93	19.2/9
1.26 ±0.01	1.25	1.86±0.04	1.86	3.12±0.11	3.13	13/10
1.29 ±0.02	1.29	1.99±0.05	2.03	3.53±0.16	3.66	16.3/10
1.295±0.008	1.294	2.01±0.03	2.04	3.58±0.09	3.72	51/11
1.30 ±0.01	1.29	2.02±0.03	2.03	3.60±0.10	3.68	29/12

TABLE II. e^+e^- annihilations. Experimental data from Ref. 6.

ISR energy (GeV)	$\langle n \rangle$	N	Dispersion D Expt.	Dispersion D Theor.	C_2 Expt.	C_2 Theor.
9.4	6.9±0.1	3	2.2±0.2	2.19	1.10±0.07	1.10
29.9–31.6	10.6±0.1	13	3.8±0.2	3.61	1.13±0.04	1.12

with our curve for fitting the e^+e^- annihilation at ISR energy 9.4 GeV. Good agreement is seen, which gives support to our view that particle production mechanisms are grossly similar for e^+e^- and $\bar{p}p$ annihilations.

V. CHARGED-PARTICLE MULTIPLICITY DISTRIBUTIONS IN MESON-PROTON COLLISIONS

To fit the inelastic topological cross sections for $\pi^\pm p$ and $K^\pm p$ collisions the model requires four parameters K_1, K_2, N_1, and N_2. However as one of the colliding particles is a proton we might expect that one set of the parameters, say K_2 and N_2, would not be very different from the parameters K and $N/2$ obtained for pp collisions.

It can be seen that the χ^2 square values are quite reasonable for beam momenta up to 200 GeV/c indicating generally good fitting. However, χ^2 per point for the fit to the higher momentum data at 250 and 360 GeV/c are rather high (about 7 per data point). Figure 4 shows the fitting KNO curves for π^-p collisions at the lowest and highest momenta fitted, 40 and 360 GeV/c. The fit is good for low and medium multiplicities. For the highest multiplicities, particularly for the higher-energy data, the model tends to give lower values than experiment. This can also be seen from Table III, where the theoretical normalized fourth mo-

TABLE III. $\pi^\pm p$ and $K^\pm p$ collisions. Experimental data from Ref. 3.

Author	Beam	Beam Momentum (GeV/c)	$\langle n \rangle$	Parameters K_1	K_2	N_1	N_2	Dispersion D Expt.	Dispersion D Theor.
Balea *et al.*	π^-	40	5.62±0.04	1	5	3	4	2.77±0.04	2.76
Akopdjanov *et al.*	π^-	50	5.78±0.04	1	6	2	4	2.70±0.03	2.70
Berger *et al.*	π^-	100	6.79±0.08	4	5	3	6	3.16±0.04	3.18
Fong *et al.*	π^-	147	7.40±0.04	6	5	3	8	3.54±0.03	3.58
Ljung *et al.*	π^-	205	7.99±0.06	14	5	3	9	3.87±0.06	3.84
Bogert *et al.*	π^-	205	8.02±0.12	14	5	3	9	3.91±0.10	3.84
Hays *et al.*	π^-	250	8.43±0.06	8	5	4	9	4.13±0.04	4.05
Firestone *et al.*	π^-	360	8.73±0.04	15	6	4	10	4.31±0.03	4.29
Akopdjanov *et al.*	π^+	50	5.89±0.06	1	5	2	3	2.58±0.04	2.61
Bromberg *et al.*	π^+	60	6.23±0.10	1	6	3	3	2.80±0.07	2.78
Morse *et al.*	π^+	100	6.62±0.07	4	5	2	7	3.19±0.05	3.18
Erwin *et al.*	π^+	100	6.80±0.14	4	5	2	7	3.30±0.13	3.21
Akopdjanov *et al.*	K^-	32	4.88±0.05	1	5	1	3	2.32±0.03	2.33
Cochet *et al.*	K^-	32	4.96±0.02	1	4	2	2	2.29±0.02	2.33
Fong *et al.*	K^-	147	7.33±0.21	2	5	3	8	3.51±0.17	3.56
Akopdjanov *et al.*	K^+	32	5.11±0.05	1	4	1	2	2.21±0.03	2.31
Morse *et al.*	K^+	100	6.65±0.31	10	5	3	7	3.34±0.19	3.31

TABLE II. *(Continued.)*

C_3		C_4		
Expt.	Theor.	Expt.	Theor.	χ^2/point
1.30±0.10	1.32	1.64±0.15	1.69	0.5/6
1.39±0.06	1.38	1.86±0.10	1.86	40.8/11

ment C_4 tends to be lower than the experimental value, though the lower moments show good agreement. This suggests that channels in addition to what are considered in the model also contribute to the production of charged particles.

The fitting parameters for the different types of meson-proton data are similar. Figure 5 shows the KNO plots for $\pi^- p$, $\pi^+ p$, and $K^+ p$ collisions at 100 GeV/c and $K^- p$ collisions at 147 GeV/c, as well as the theoretical curves for $\pi^- p$ and $K^- p$ collisions at 100 GeV/c. The agreement among the data is remarkable. This agreement is reflected in the closeness of the two theoretical curves.

It is interesting to compare the KNO curves from our model for pp and $\pi^- p$ collisions at the same beam momentum. The theoretical curves for such collisions at 205 GeV/c as well as the experimental data from Charlton *et al.*[12] and Bogert *et al.*[3] are shown in Fig. 6.

VI. DISCUSSION

We have been able to fit the available high-energy topological cross section data from pp, e^+e^-, and $\bar{p}p$ interactions in terms of a single model—the MTC model. The only empirical input is the mean charged-particle multiplicity $\langle n \rangle$. As K is only mildly energy dependent, there is essentially only one free parameter to be fitted, the

TABLE III. *(Continued.)*

C_2		C_3		C_4		
Expt.	Theor.	Expt.	Theor.	Expt.	Theor.	χ^2/point
1.24 ±0.03	1.24	1.82±0.05	1.80	3.05±0.13	2.95	4.1/9
1.22 ±0.02	1.22	1.72±0.04	1.71	2.71±0.07	2.70	19.8/8
1.22 ±0.02	1.22	1.71±0.04	1.71	2.71±0.08	2.69	11.6/9
1.23 ±0.02	1.23	1.75±0.03	1.76	2.82±0.07	2.79	47/11
1.23 ±0.03	1.23	1.77±0.06	1.74	2.84±0.13	2.71	30.9/10
1.24 ±0.04	1.23	1.78±0.08	1.73	2.86±0.15	2.70	18.2/11
1.240±0.005	1.231	1.80±0.02	1.75	2.98±0.06	2.77	83.1/14
1.244±0.003	1.242	1.80±0.01	1.78	2.94±0.04	2.81	88.8/14
1.20 ±0.02	1.20	1.65±0.04	1.63	2.52±0.08	2.47	21.2/8
1.20 ±0.05	1.20	1.65±0.09	1.64	2.52±0.17	2.51	4.6/8
1.23 ±0.03	1.23	1.77±0.06	1.75	2.84±0.12	2.76	8.8/10
1.24 ±0.04	1.22	1.78±0.08	1.72	2.87±0.18	2.69	12.9/9
1.23 ±0.03	1.23	1.74±0.05	1.74	2.76±0.09	2.75	3.8/7
1.21 ±0.01	1.22	1.69±0.03	1.71	2.64±0.06	2.68	23.1/7
1.23 ±0.11	1.24	1.78±0.20	1.79	2.96±0.43	2.93	11.2/9
1.20 ±0.02	1.20	1.63±0.04	1.65	2.48±0.07	2.52	16.3/7
1.25 ±0.12	1.25	1.84±0.24	1.80	3.05±0.54	2.88	4.3/7

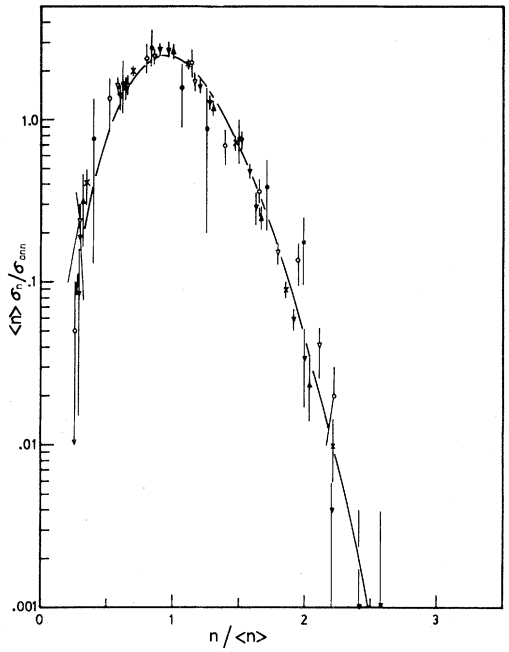

FIG. 3. KNO plots for $\bar{p}p$ annihilations, σ_{ann} being the total annihilation cross section. Experimental points [(compiled by Rushbrooke *et al.*[7] (Ref. 7)]. ● 100 GeV/c ($\bar{p}p - pp$), ○ 32 GeV/c ($\bar{p}p - pp$), ∇ 22.4 GeV/c ($\bar{p}p - pp$), ▼ 14.75 GeV/c ($\bar{p}p - pp$), ▲ 12 GeV/c ($\bar{p}p - pp$), × 9 GeV/c (annihilation). Solid curve is the theoretical curve fitting e^+e^- annihilations at 9.4 GeV ISR.

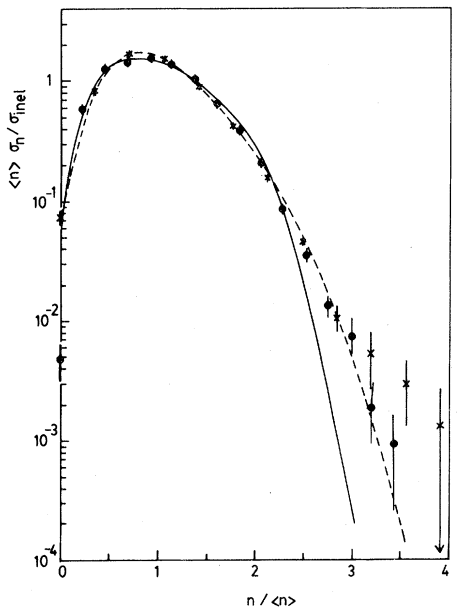

FIG. 4. KNO plots for π^-p collisions. × 40 GeV/c, ● 360 GeV/c. Fitting curves: dashed 40 GeV/c, continuous 360 GeV/c.

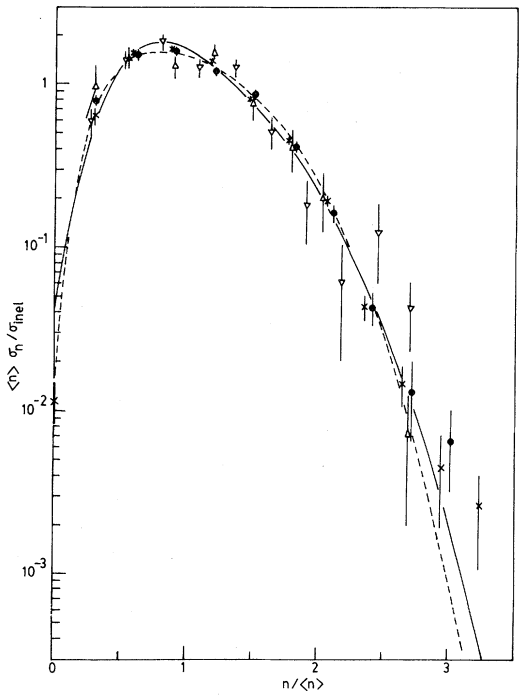

FIG. 5. KNO plots for collisions at beam momenta 100 GeV/c (× π^-p, ● π^+p, △ K^+p) and 147 GeV/c (∇ K^-p). The theoretical curves are for π^-p (continuous) and K^+p collisions (dashed) at 100 GeV/c.

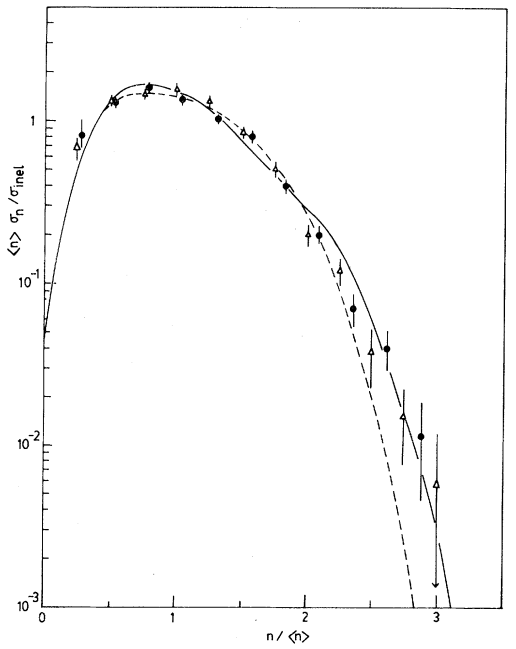

FIG. 6. KNO plots for pp collisions ● [Charlton *et al.* (Ref. 12)] and π^-p collisions △ [Bogert *et al.* (Ref. 3)] for beam momentum 205 GeV/c. Fitting curves: continuous pp, dashed π^-p.

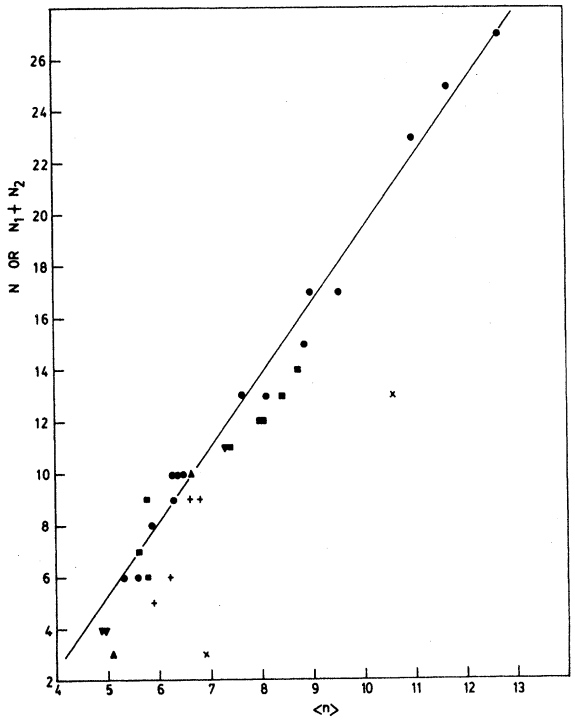

FIG. 7. Fragmentation cutoff N or N_1+N_2 versus mean charged multiplicity $\langle n \rangle$. ● pp, ■ $\pi^- p$, $+\pi^+ p$, ▼ $K^- p$, ▲ $K^+ p$ collisions; × e^+e^- annihilations. The straight line is the best-fit line for pp collisions.

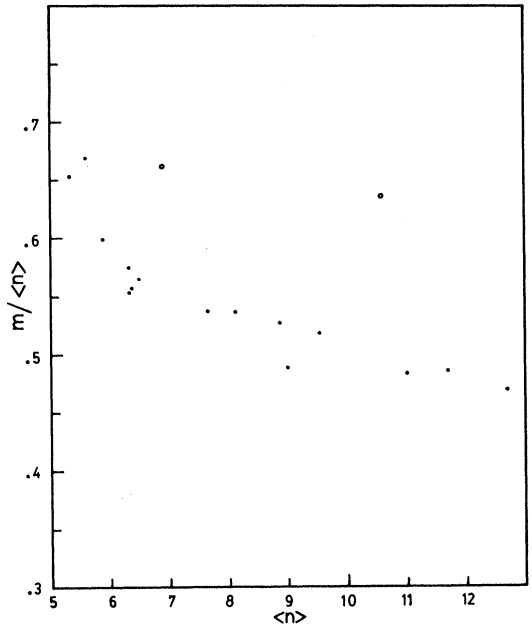

FIG. 8. $m/\langle n \rangle$ versus $\langle n \rangle$. ● pp collisions, ○ e^+e^- annihilations.

fragmentation cutoff N. Figure 7 shows the variation of N with $\langle n \rangle$ for the pp collision data. These may be fitted with a linear equation

$$N = 2.84\langle n \rangle - 8.96 \, .$$

The total fragmentation limits N_1+N_2 for the meson-proton collision data are also plotted in the same figure.

In the MTC model, the processes of pionization and fragmentation are mixed in the sense that charge conservation applies to the interaction as a whole; they are otherwise independent. This would imply some kind of underlying long-range interaction. A more acceptable alternative is that the charges of the excited hadrons are determined during excitation, with diffractive fragmentation following. A matter of some interest is the relative contributions of the nondiffractive pionization and the fragmentation to the mean multiplicity in the MTC model. Figure 8 shows the ratio $m/\langle n \rangle$, where m is the contribution of the central region as defined by Eq. (6), as a function of $\langle n \rangle$ for pp collisions and e^+e^- annihilations. The ratio decreases from about 0.65 to 0.5 as $\langle n \rangle$ increases from 5 to 13 for pp collisions.

---

[1] pp inelastic topological cross sections at different beam momenta: 50 GeV/c: V. V. Ammosov *et al.*, Phys. Lett. 42B, 519 (1972); 60 GeV/c: C. Bromberg *et al.*, Phys. Rev. D 15, 64 (1977); 69 GeV/c: V. V. Ammosov, Phys. Lett. 42B, 519 (1972); 100 GeV/c: J. Erwin *et al.*, Phys. Rev. Lett. 32, 254 (1974); W. M. Morse *et al.*, Phys. Rev. D 15, 66 (1977); 102 GeV/c: J. W. Chapman *et al.*, Phys. Rev. Lett. 29, 1686 (1973); C. Bromberg *et al.*, *ibid.* 31, 1563 (1973); 205 GeV/c: G. Charlton *et al.*, *ibid.* 29, 515 (1972); 303 GeV/c: F. T. Dao *et al.*, *ibid.* 29, 627 (1972); 405 GeV/c: C. Bromberg *et al.*, *ibid.* 31, 1563 (1973).

[2] W. Thomé *et al.*, Nucl. Phys. B129, 365 (1977).

[3] Inelastic topological cross sections for $\pi^- p$ collisions at various beam momenta: 40 GeV/c: O. Balea *et al.*, Phys. Lett. 39B, 571 (1972); 50 GeV/c: G. A. Akopdjanov *et al.*, Nucl. Phys. B75, 401 (1974); 100 GeV/c: E. L. Berger *et al.*, *ibid.* B77, 365 (1974); 147 GeV/c: D. Fong *et al.*, *ibid.* B102, 386 (1976);

205 GeV/c: D. Ljung *et al.*, Phys. Rev. D 15, 3163 (1977); D. Bogert *et al.*, Phys. Rev. Lett. 31, 1271 (1973); 250 GeV/c: P. J. Hays *et al.*, report (unpublished); 360 GeV/c: A. Firestone *et al.*, Phys. Rev. D 14, 2902 (1976). π^+p collisions at various beam momenta: 50 GeV/c: G. A. Akopdjanov *et al.*, Nucl. Phys. B75, 401 (1974); 60 GeV/c: C. Bromberg *et al.*, Phys. Rev. D 15, 64 (1977); 100 GeV/c: W. M. Morse *et al., ibid.* 15, 66 (1977); J. Erwin *et al.*, Phys. Rev. Lett. 32, 254 (1974). K^-p collisions at various beam momenta: 32 GeV/c: G. A. Akopdjanov *et al.*, Nucl. Phys. B75, 401 (1974); C. Cochet *et al., ibid.* B124, 61 (1977); 147 GeV/c: D. Fong *et al., ibid.* B102, 386 (1976). K^+p collisions at various beam momenta: 32 GeV/c: G. A. Akopdjanov *et al., ibid.* B75, 401 (1974); 100 GeV/c; W. M. Morse *et al.*, Phys. Rev. D 15, 66 (1977).

[4]Z. Koba, H. B. Nielsen, and P. Olesen, Nucl. Phys. B40, 317 (1972).

[5]P. Slattery, Phys. Rev. Lett. 29, 1624 (1972).

[6]Ch. Berger, Phys. Lett. 95B, 313 (1980).

[7]J. R. Rushbrooke *et al.*, Phys. Lett. 59B, 303 (1975).

[8]C. H. Kam, H. B. Low, and K. K. Phua, Nuovo Cimento 31A, 356 (1976).

[9]L. van Hove and M. Jacob, Phys. Rep. 62, 1 (1980).

[10]C. Quigg, J. M. Wong, and C. N. Yang, Phys. Rev. Lett. 28, 1290 (1972).

[11]E. Segrè, *Nuclei and Particles,* 2nd Edition (W. A. Benjamin, Reading, Massachusetts, 1977).

[12]G. Charlton *et al.*, Phys. Rev. Lett. 29, 515 (1972).